JOURNAL OF BACTERIOLOGY, Apr. 2011, p. 1911–1918 Vol. 193, No. 8
0021-9193/11/$12.00 doi:10.1128/JB.01317-10

The Interplay of ClpXP with the Cell Division Machinery in *Escherichia coli*▽†

Jodi L. Camberg, Joel R. Hoskins, and Sue Wickner*

Laboratory of Molecular Biology, National Cancer Institute, National Institutes of Health, Bethesda, Maryland 20892

Received 30 October 2010/Accepted 3 February 2011

ClpXP is a two-component protease composed of ClpX, an ATP-dependent chaperone that recognizes and unfolds specific substrates, and ClpP, a serine protease. One ClpXP substrate in *Escherichia coli* is FtsZ, which is essential for cell division. FtsZ polymerizes and forms the FtsZ ring at midcell, where division occurs. To investigate the role of ClpXP in cell division, we examined the effects of *clpX* and *clpP* deletions in several strains that are defective for cell division. Together, our results suggested that ClpXP modulates cell division through degradation of FtsZ and possibly other cell division components that function downstream of FtsZ ring assembly. In the *ftsZ84* strain, which is temperature sensitive for filamentation due to a mutation in *ftsZ*, we observed that deletion of *clpX* or *clpP* suppresses filamentation and reduces FtsZ84 degradation. These results are consistent with ClpXP playing a role in cell division by modulating the level of FtsZ through degradation. In another division-defective strain, Δ*minC*, the additional deletion of *clpX* or *clpP* delays cell division and exacerbates filamentation. Our results demonstrate that ClpXP modulates division in cells lacking MinC by a mechanism that requires ATP-dependent degradation. However, antibiotic chase experiments *in vivo* indicate that FtsZ degradation is slower in the Δ*minC* strain than in the wild type, suggesting there may be another cell division component degraded by ClpXP. Taken together these studies suggest that ClpXP may degrade multiple cell division proteins, thereby modulating the precise balance of the components required for division.

The cell division machinery in *Escherichia coli* is responsible for the constriction and separation of a mother cell into two daughter cells. Many proteins spatially and temporally coordinate their activities to complete division in an efficient manner. The major structural component is FtsZ, a tubulin-like protein that assembles into a circumferential ring, termed the FtsZ ring, at midcell, the site of cell division (1). FtsZ polymerizes in a reaction requiring GTP binding but not hydrolysis. *In vitro*, FtsZ forms a range of structures, including single-stranded protofilaments, bundles, tubules, and sheets, depending on the experimental conditions used. However, the architecture of the FtsZ ring that is formed *in vivo* is not fully understood. Results from electron cryotomography studies of dividing cells suggest the FtsZ ring consists of short overlapping protofilaments rather than a continuous ring (27). *In vitro* and *in vivo* FtsZ polymers undergo dynamic disassembly and reassembly, which are coupled to GTP binding and hydrolysis by FtsZ (4, 12).

Proper placement of the FtsZ ring at midcell is regulated by several factors. One regulatory system in *E. coli* is the Min system, comprised of MinC, MinD, and MinE (28). The Min system promotes formation of the FtsZ ring at midcell by preventing its formation near the poles. MinC interacts directly with FtsZ and inhibits FtsZ polymerization (16). MinD, a membrane-associated ATPase, recruits MinC to the membrane, where it antagonizes FtsZ assembly. The function of MinC/MinD is controlled by MinE. MinE stimulates ATPase activity of MinD and promotes dissociation of MinD complexes from the membrane (25, 26). MinC and MinD are observed to oscillate between the two poles, inhibiting FtsZ ring formation near the poles and thereby preventing anucleate cells (29). In strains deleted for *minC* alone, or the full *minCDE* operon, cell division occurs; however, the FtsZ ring is misplaced, causing minicells, elongated cells, and short filaments to form (2, 17, 40). A second regulator of FtsZ ring position is a nucleoid occlusion factor, SlmA in *E. coli* (8). It prevents the assembly of the FtsZ ring over the nucleoid *in vivo* (8). *In vitro*, SlmA binds directly to FtsZ, likely altering the arrangement of FtsZ protofilaments (35).

An additional regulator of FtsZ that has been identified is ClpX (11, 34, 38). ClpX is a member of the AAA+ (ATPases associated with various cellular activities) family of ATPases and forms a complex with ClpP, a serine protease. ClpX recognizes substrates harboring ClpX recognition motifs or an SsrA tag and catalyzes ATP-dependent unfolding of the polypeptide and transfer of the unfolded protein into the cavity of ClpP for degradation (32). In *Bacillus subtilis*, the Levin group found that *in vivo* ClpX helps regulate cell division and that *in vitro* it inhibits FtsZ polymerization in an ATP- and ClpP-independent fashion (22, 38). Recently, it has been shown that ClpX also modulates cell division in *Mycobacterium tuberculosis*, possibly by an ATP-independent mechanism (18).

In *E. coli*, FtsZ was discovered to be associated with ClpXP protease in a proteomic study aimed at identifying ClpXP substrates (19). Subsequently, it was found that ClpXP degrades FtsZ in *E. coli*, but only 10 to 15% is turned over per cell cycle (11). Overproduction of both ClpX and ClpP ex-

* Corresponding author. Mailing address: 37 Convent Drive, Room 5144, National Cancer Institute, National Institutes of Health, Bethesda, MD 20892. Phone: (301) 496-2629. Fax: (301) 402-1344. E-mail: WicknerS@mail.nih.gov.

† Supplemental material for this article may be found at http://jb.asm.org/.

▽ Published ahead of print on 11 February 2011.

TABLE 1. *E. coli* strains and plasmids used in this study

Strain or plasmid	Genotype[a]	Source, reference, or construction[b]
E. coli strains		
BW25113	Δ(*araD-araB*)*567* Δ*lacZ4787*(::*rrnB-3*) λ⁻ *rph-1* Δ(*rhaD-rhaB*)*568 hsdR514*	5
JW1165	BW25113 Δ*minC765*::*kan*	5
JW0428	BW25113 Δ*clpX724*::*kan*	5
JW0427	BW25113 Δ*clpP723*::*kan*	5
MG1655	λ⁻ *rph-1*	10
JC0232	MG1655 Δ*minC*::*frt*	P1(JW1165) × MG1655; pCP20
JC0259	MG1655 Δ*clpX*::*kan*	P1(JW0428) × MG1655
JC0263	MG1655 Δ*clpP*::*kan*	P1(JW0427) × MG1655
JC0292	MG1655 Δ*minC*::*frt* Δ*clpX*::*frt*	P1(JW0428) × JC0232; pCP20
JC0302	MG1655 Δ*minC*::*frt* Δ*clpP*::*kan*	P1(JW0427) × JC0232
MCZ84	[*araD139*] *leu-260*::Tn*10 ftsZ84*(Ts) Δ(*argF-lac*)*169* λ⁻ *e14*⁻ *flhD5301* Δ(*fruK-yeiR*)*725*(*fruA*) *relA1 rpsL150*(Str^r) *rbsR22* Δ(*fimB-fimE*)*632*(::IS*1*) *deoC1*	15
JC0303	MCZ84 Δ*clpX*::*kan*	P1(JW0428) × MCZ84
JC0304	MCZ84 Δ*clpP*::*kan*	P1(JW0427) × MCZ84
Plasmids		
pCP20	*amp flp* recombinase	13
pBAD24	*amp* (expression vector)	21
pClpX	*amp* P_{ara}::*clpX*	This study
pClpX(E185Q)	*amp* P_{ara}::*clpX*(E185Q)	This study
pClpP	*amp* P_{ara}::*clpP*	This study
pGfp-FtsZ	*amp* P_{ara}::*gfp-ftsZ*	This study
pClpXP	*amp* P_{clpP}::*clpPX*	11

[a] The *kan* cassette is flanked by *frt* sites for removal by FLP recombinase. An *frt* scar remains after removal of the cassette by using FLP expressed from pCP20.
[b] Strain constructions by P1 transduction are described as the P1(donor) × the recipient. Where indicated, removal of the Kan cassette (by use of pCP20) is noted.

pressed from the natural promoter by using a multicopy plasmid caused an increase in the rate of FtsZ degradation and a filamentous phenotype (11). The same study showed that ClpXP degrades both FtsZ monomers and polymers *in vitro* (11). In a subsequent study it was reported that overexpression of either full-length ClpX or the N-terminal substrate binding domain of ClpX to very high levels causes filamentation and perturbs formation of the FtsZ ring in a wild-type background (34). It was also reported that *in vitro* ClpX could inhibit FtsZ polymerization by an ATP- and ClpP-independent mechanism (34).

To investigate how protein degradation by ClpXP modulates cell division in *E. coli*, we examined the effects of *clpX* and *clpP* deletions in several strains defective in cell division at the level of the FtsZ ring. We observed that deletion of *clpX* and *clpP* suppresses temperature-sensitive filamentation of cells carrying the *ftsZ84* allele and reduces FtsZ84 degradation, consistent with ClpXP playing a role in modulating the level of FtsZ. In a *minC* deletion strain, in which the majority of cells contain multiple FtsZ rings, the additional deletion of either *clpX* or *clpP* delays cell division and causes enhanced filamentation; however, FtsZ turnover is decreased in both Δ*minC* and Δ*clpX* Δ*minC* strains compared to the wild type. Our results show that ClpXP affects cell division by a mechanism that requires ATP-dependent degradation, suggesting that ClpXP modulates the balance of cell division proteins.

MATERIALS AND METHODS

Bacterial strains and plasmids. *E. coli* strains and plasmids used in this study are listed in Table 1. Bacteria were grown in Luria-Bertani (LB) liquid broth at 30°C. *E. coli* strains containing full in-frame insertion-deletions for *clpX*, *clpP*, and *minC* were acquired from the Keio Collection (5). Deletion mutations were brought into MG1655 by P1 transduction. To construct multiple deletion sets, we first removed the kanamycin cassettes from our single-deletion strains by transformation with pCP20 to provide the FLP recombinase (13), and then strains were cured of pCP20 by a temperature upshift to 42°C. The cured strains were transduced again with P1 lysate prepared from a different deletion strain.

The genes for *clpX*, *clpP*, and *ftsZ* were amplified by PCR and cloned into expression vector pBAD24. *ftsZ* was cloned into expression vector pBAD-GFP(uv) (24) at the 3′ end of the *gfp* sequence by using the restriction sites SacI and PstI to create pGfp-FtsZ. Site-directed mutagenesis of pClpX was performed to construct pClpX(E185Q) by using the QuikChange II kit (Stratagene). To test for complementation, plasmid-containing cells were grown overnight in LB medium with ampicillin (100 μg ml^{-1}) and arabinose (0.05% or 0.1% for strains containing pClpX or pClpP, respectively). Cells were diluted into fresh medium to an optical density at 600 nm (OD_{600}) of 0.01 and then grown at 30°C. At an OD_{600} of ~0.4, cells were examined by microscopy. Expression levels of ClpX, ClpX(E185Q), and ClpP were verified by immunoblotting.

Microscopy and immunofluorescence. Overnight cultures were diluted into LB broth to an OD_{600} of 0.01 and grown at 30°C for 3 h. Where indicated, cells from an overnight culture grown in LB were diluted into M63 minimal medium with 0.2% glucose to an OD_{600} of 0.01, and grown at 30°C for 6 h. Cells were collected by centrifugation at 600 × *g* for 5 min and washed in ice-cold phosphate-buffered saline (PBS) with 1 mM EDTA. Cells were applied to a glass slide, and a poly-L-lysine coated coverslip was added.

To observe the location of FtsZ rings in live cells, we expressed Gfp-FtsZ in strains carrying the expression plasmid pGfp-FtsZ by growing the cells at 30°C in arabinose (0.015%) and ampicillin (100 μg ml^{-1}). Log-phase cells were prepared as described above and examined immediately by fluorescence microscopy.

Cells were imaged by differential interference contrast (DIC) microscopy by using a Nomarski prism and by fluorescence microscopy using an Axio Imager M2 microscope (Zeiss) with an αPlan-Apochromat 100×/1.46-numerical aperture oil objective and the filter sets 4′,6-diamidino-2-phenylindole (DAPI) and fluorescein. Pictures were taken with an Axiocam camera. Images were processed using Adobe Photoshop CS3 and analyzed using NIH ImageJ software.

Protein turnover experiments. *E. coli* strains were grown in LB at 30°C to the specified OD_{600} (0.3 to 0.5). To inhibit protein synthesis, spectinomycin was added to the cultures to a final concentration of 200 μg ml^{-1}, and cell extracts were prepared at 1-h intervals after the addition of spectinomycin, as described previously (11). FtsZ turnover was monitored by immunoblotting with FtsZ antibodies as described previously (11). A minimum of three replicates was performed.

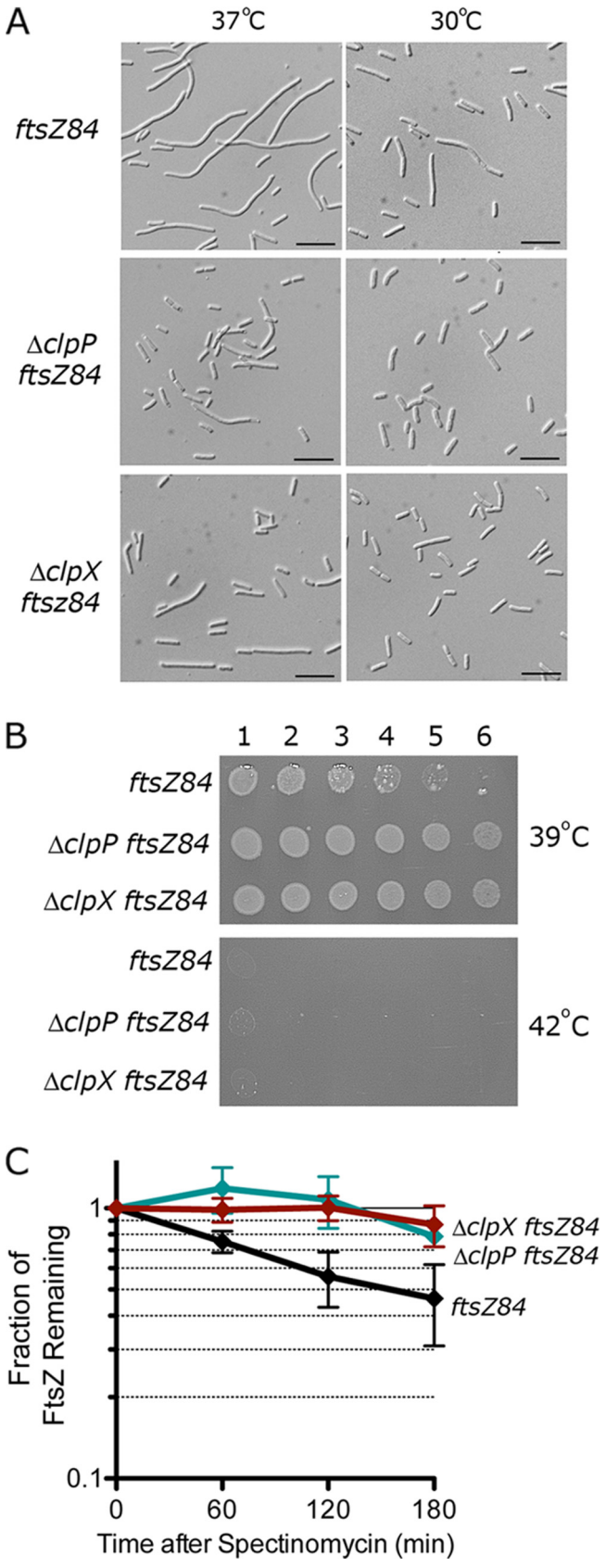

FIG. 1. Deletion of *clpP* or *clpX* suppresses temperature-sensitive filamentation in cells carrying the FtsZ84 mutation. (A) *ftsZ84* (MCZ84), Δ*clpP ftsZ84* (JC0304), and Δ*clpX ftsZ84* (JC0303) cells were grown at 30°C and 37°C to an OD_{600} of 0.5 and analyzed by DIC microscopy. Median cell lengths ($n = 200$) at 30°C for each strain were 3.6 μm ± 0.1 (Δ*clpP ftsZ84*), 3.5 μm ± 0.1 (Δ*clpX ftsZ84*), and 4.4 μm (*ftsZ84*). Bars, 10 μm. (B) Log dilutions of cultures grown overnight at 30°C that were then spotted onto LB plates. Plates were incubated overnight at 39°C and 42°C. (C) FtsZ84 turnover was monitored in cultures of *ftsZ84*, Δ*clpP ftsZ84*, and Δ*clpX ftsZ84* strains grown at 30°C in LB after addition of spectinomycin. The relative change in FtsZ84 band intensity was monitored by immunoblotting with FtsZ antibodies.

RESULTS AND DISCUSSION

Blocking protein degradation by ClpXP suppresses filamentation of *ftsZ84*. Elevated levels of ClpXP increase FtsZ degradation *in vivo* and cause cellular filamentation (11), suggesting that ClpXP may influence cell division by modulating the intracellular concentration of FtsZ. The *ftsZ84* strain carries a glycine-to-serine substitution mutation at amino acid position 105 of FtsZ (9). These cells divide normally at 28°C but form filaments at 37°C and are nonviable at 42°C (9). It has been shown that these phenotypes can be suppressed by increasing the intracellular FtsZ84 concentration (36). Therefore, to determine if protein degradation is also involved in limiting the amount of FtsZ84 available in the *ftsZ84* temperature-sensitive strain (MCZ84), we deleted *clpP* and *clpX* and tested for suppression of temperature-sensitive filamentation.

When we compared cellular morphology of *ftsZ84* (MCZ84), Δ*clpP ftsZ84* (JC0304), and Δ*clpX ftsZ84* (JC0303) strains at 37°C, we saw that the *ftsZ84* cells formed long filaments, as observed previously (Fig. 1A). In contrast, Δ*clpP ftsZ84* and Δ*clpX ftsZ84* cells formed elongated rods and short filaments at 37°C (Fig. 1A). A difference in cell length was also observed at 30°C between *ftsZ84* cells and the double mutants, Δ*clpP ftsZ84* and Δ*clpX ftsZ84* (Fig. 1A); the cells of the double mutants were ~20% shorter than *ftsZ84* cells.

To determine if deletion of either *clpP* or *clpX* restored viability of *ftsZ84* at 42°C, the nonpermissive temperature, we grew these strains in liquid LB at 30°C and then plated the cultures onto LB plates. While none of these strains grows at 42°C, deletion of either *clpP* or *clpX* enhanced viability at 39°C (Fig. 1B). These results indicate that deletion of either *clpP* or *clpX* partially suppresses the temperature-sensitive phenotype caused by the chromosomal *ftsZ84* mutation.

We next tested if degradation of FtsZ84 is reduced in Δ*clpP ftsZ84* and Δ*clpX ftsZ84* strains by monitoring FtsZ84 turnover by immunoblotting after halting protein synthesis. We calculated that the half-life of FtsZ84 is ~150 min, and deletion of *clpP* or *clpX* prevents degradation of FtsZ84 (Fig. 1C). Our results suggest that deletion of *clpP* or *clpX* suppresses temperature-sensitive filamentation by decreasing FtsZ84 protein turnover.

Aberrant division in *clp min* double mutants. Degradation of FtsZ modulates cell division in wild-type (11) and *ftsZ84* (Fig. 1) strains. ClpX, with and without ClpP, functions as a negative regulator of FtsZ assembly *in vitro*, yet ClpP and ClpX are not essential proteins in *E. coli* (20). We hypothesized that in the absence of the main negative regulator of FtsZ assembly in the cell, MinC, ClpXP may play a more important role in cell

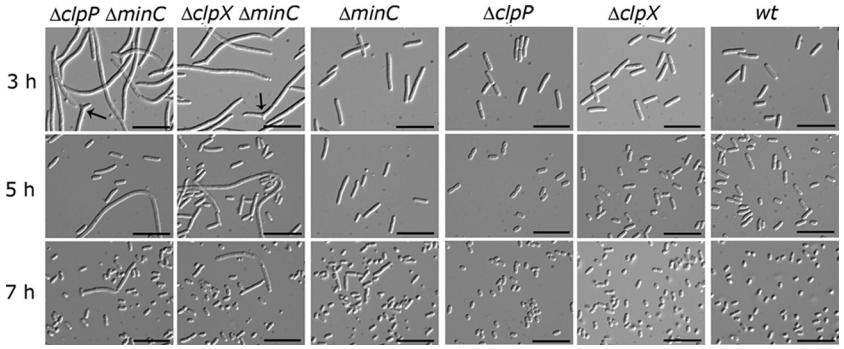

FIG. 2. Deletion of *clpP* or *clpX* in the *minC* deletion strain exacerbates cellular filamentation. Δ*clpP* Δ*minC* (JC0302), Δ*clpX* Δ*minC* (JC0292), Δ*minC* (JC0232), Δ*clpP* (JC0263), Δ*clpX* (JC0259), and wild-type (wt; MG1655) cells were grown at 30°C. Live cells were analyzed by DIC microscopy after growth for 3 h, 5 h, and 7 h as described in Materials and Methods. Arrows point to branches. Bars, 10 μm.

division. To address this we constructed double deletions of either *clpP* or *clpX* with *minC* and examined cell length by microscopy.

As previously seen (17), we observed that deletion of *minC* caused cells to divide asymmetrically, resulting in short filaments, elongated rods, and minicells (Fig. 2). Short filaments produced by the Δ*minC* strain were approximately 2- to 3-fold longer than cells produced by the wild-type strain. When we examined cells from exponentially growing cultures (OD_{600}, ~0.3; 3 h of growth) of both the *clpP minC* (JC0302) and the *clpX minC* (JC0292) double deletion strains, we observed severe defects in cell division (Fig. 2). Cultures of both Δ*clpP* Δ*minC* and Δ*clpX* Δ*minC* strains contained very long filamentous cells, in contrast to the short filaments and elongated cells of the Δ*minC* culture. Numerous long filaments observed in the double deletion strains were ~10-fold longer than those of a wild-type *E. coli* cell, and some filaments were branched (Fig. 2). Two percent of the filaments in cultures of Δ*clpP* Δ*minC* and Δ*clpX* Δ*minC* strains were branched when cells were grown in LB broth (Fig. 2). Branches were not observed in cultures of wild-type cells or any of the strains carrying a single deletion. Branching has previously been observed in cells carrying the *minCDE* triple deletion under certain conditions and in combination with *ftsZ84* (3, 39). The number of minicells in all strains carrying the *minC* deletion was similar (~25%) with respect to the total number of cells in each culture, regardless of length. Deletion of either *clpP* (JC0263) or *clpX* alone (JC0259) did not induce filamentation, and these cells appeared similar to wild-type cells (MG1655), as previously reported (11, 20) (Fig. 2). Our results suggest that in the absence of ClpXP protease, a *minC* deletion causes extensive cellular filamentation.

We continued to monitor cell length as cells progressed through exponential phase to determine if the Δ*clpP* Δ*minC* and Δ*clpX* Δ*minC* cells were blocked or delayed for cell division. Compared to the large number of filamentous cells seen during exponential growth of Δ*clpP* Δ*minC* and Δ*clpX* Δ*minC* cells, many fewer filaments were seen in the cultures after 5 h of growth, as cells approached stationary phase (Fig. 2; see also Fig. S1A in the supplemental material). After 7 h, the majority of cells in both cultures began to acquire a smaller round appearance typical of stationary-phase wild-type and Δ*minC* cells (Fig. 2). By this time, only a few relatively short filaments remained in the Δ*clpP* Δ*minC* and Δ*clpX* Δ*minC* strains. Since colony formation of all strains was similar after cells reached stationary phase (see Fig. S1B), our results suggest that the filaments seen in exponential phase undergo division, resulting in viable cells.

Cell division and cell growth are coordinately regulated based on nutrient availability (37). Slowing cell growth can overcome certain cell division delays, allowing cells more time to complete a division cycle. Culturing cells in minimal medium suppresses filamentation of Δ*slmA* Δ*minCDE* cells (8). Therefore, to determine if slow cell growth also suppresses filamentation of Δ*clpX* Δ*minC* and Δ*clpX* Δ*minC* cells, we grew these strains in M63 minimal medium with glucose (0.2%). Cultures of Δ*clpX* Δ*minC* and Δ*clpP* Δ*minC* cells grown in minimal medium were not filamentous and were similar in length to Δ*minC* cells (see Fig. S2 in the supplemental material).

Our results indicate that in the absence of MinC and either ClpX or ClpP, there is a profound delay in the time required to complete division when cells are grown in nutrient-rich medium. They further suggest that in the absence of MinC, ClpXP promotes FtsZ ring constriction. The observation that deletion of *minC* is more detrimental in a Δ*clpX* or Δ*clpP* strain implies that MinC and ClpXP have an overlapping function during division, although the mechanisms by which they carry out this function would undoubtedly be different.

ATP-dependent protein unfolding and proteolysis by ClpXP are essential for promoting FtsZ ring constriction in the *minC* mutant. The previous result suggested that ClpXP may perform an overlapping function with MinC to promote cell division. To determine if the filamentous phenotype in the Δ*clpX* Δ*minC* strain could be rescued by the addition of ClpX, we expressed *clpX* from a plasmid under the control of the arabinose-inducible promoter and observed the cells by microscopy. The majority of Δ*clpX* Δ*minC* cells expressing *clpX* from a plasmid were short filaments (Fig. 3A and B), similar to the short filaments observed for the Δ*minC* strain (Fig. 2). The majority of Δ*clpX* Δ*minC* cells carrying the control vector were very long filaments (Fig. 3A). In control experiments, we observed that the overexpression of ClpX driven by the arabinose-inducible promoter did not cause filamentation in the wild-type *E. coli* strain MG1655 (see Fig. S3 in the supplemental material). Together, the results show that the lack of ClpX

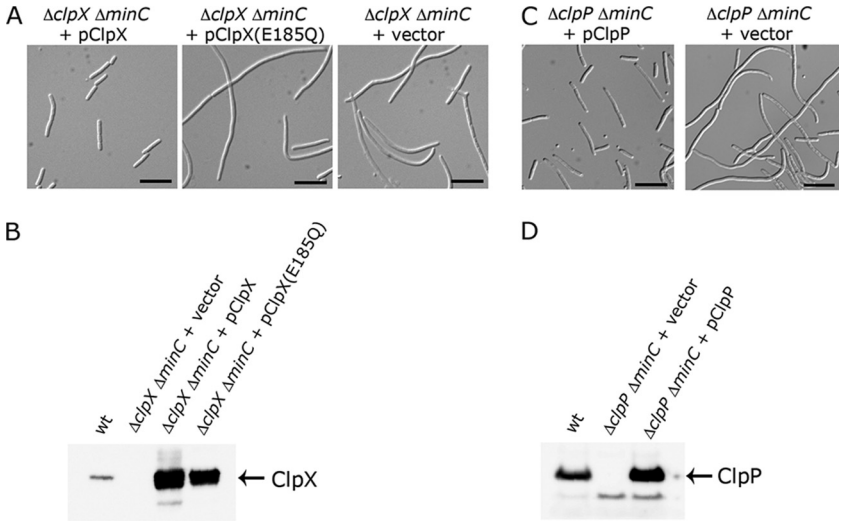

FIG. 3. Suppression of long filaments in the Δ*clpX* Δ*minC* and Δ*clpP* Δ*minC* strains. (A) Δ*clpX* Δ*minC* (JC0292) cells containing pClpX, pClpX(E185Q), or control vector pBAD24 were grown at 30°C to an OD_{600} of ~0.4 in the presence of arabinose (0.05%) and ampicillin (100 μg ml^{-1}) and then visualized by DIC microscopy. Bars, 10 μm. (B) Extracts of wild-type (MG1655) or Δ*clpX* Δ*minC* cells expressing ClpX or ClpX(E185Q) were immunoblotted with antibodies to ClpX. (C) Δ*clpP* Δ*minC* (JC0302) cells containing pClpP or pBAD24 were grown and visualized as described above except the medium contained 0.1% arabinose. Bars, 10 μm. (D) Extracts of wild-type (MG1655) or Δ*clpP* Δ*minC* cells expressing ClpP were immunoblotted with antibodies to ClpP.

is responsible for the cell division delay in the Δ*clpX* Δ*minC* strain.

We next tested whether the ATP-dependent protein unfolding activity of ClpX is required to prevent the formation of long filaments in the Δ*minC* strain. To do this we analyzed cells following expression of a ClpX mutant with an amino acid substitution in the Walker B nucleotide binding motif, ClpX(E185Q). This mutation blocks the ability of ClpX to hydrolyze ATP, thus preventing ATP-dependent unfolding by ClpX (23). When plasmid-encoded ClpX(E185Q) was expressed in the Δ*clpX* Δ*minC* double deletion strain, we observed long filamentous cells similar to those seen in the double deletion strain carrying the empty vector (Fig. 3A). Expression of ClpX(E185Q) was verified by immunoblot analysis (Fig. 3B). Importantly, these results demonstrated that ATP hydrolysis by ClpX is required for the function of ClpX during cell division in Δ*minC* cells.

To determine whether ClpP suppresses the filamentous phenotype in the Δ*clpP* Δ*minC* double mutant, we expressed *clpP* from a plasmid under the control of the arabinose-inducible promoter and examined the cells by microscopy (Fig. 3C). We observed that the majority of cells expressing ClpP from a plasmid were short filaments or elongated rod-shaped cells, in contrast to the long filamentous cells carrying the control vector, indicating that the long filament phenotype in the Δ*clpP* Δ*minC* strain is suppressed by plasmid-encoded ClpP. Expression of ClpP was verified by immunoblot analysis (Fig. 3D). Taken together, our results show that both ClpX and ClpP are important for promoting cell division in the Δ*minC* strain. The results suggest that ATP-dependent degradation by ClpXP modulates cell division in Δ*minC* cells.

FtsZ localizes to rings, but the rings are slow to constrict in Δ*clpP* Δ*minC* and Δ*clpX* Δ*minC* cells. A cell division delay suggests that Δ*clpP* Δ*minC* and Δ*clpX* Δ*minC* cells may be defective in assembly of the FtsZ ring, constriction, or septation. To visualize the ring, we expressed Gfp-FtsZ from a vector under the control of the arabinose promoter to a level that was approximately 30% of the total cellular FtsZ (see Fig. S4 in the supplemental material) and observed live cells by fluorescence microscopy. Δ*clpX* Δ*minC* and Δ*clpP* Δ*minC* cells showed fluorescent FtsZ rings that appeared similar to the FtsZ rings in Δ*minC* cells (Fig. 4). Similar results were obtained by immunofluorescence detection of native FtsZ (see Fig. S5 in the supplemental material). We occasionally observed thick or double FtsZ rings in all strains deleted for *minC* (Fig. 4; see also Fig. S5). We also observed variations in FtsZ ring intensity and frequency along the length of the filament in all cells deleted for *minC*; a similar observation was made previously in filamentous cells deleted for *minCDE* (40). The Δ*clpP* Δ*minC* and the Δ*clpX* Δ*minC* strains as well as the Δ*minC* strain had approximately twice as many FtsZ rings per unit length as the wild-type cells (see Fig. S5), consistent with previously reported results in Δ*minCDE* cells (8). DNA staining with DAPI showed that FtsZ rings are positioned between nucleoids in Δ*minC*, Δ*clpP* Δ*minC*, and Δ*clpX* Δ*minC* cells (see Fig. S5). Our results show that although the Δ*clpX* Δ*minC* and Δ*clpP* Δ*minC* filaments are delayed for division, FtsZ rings form at intervals poised to participate in dividing the filament into many rod-shaped cells.

FtsZ degradation is slowed in Δ*minC* cells. Since we previously observed that ClpXP degrades FtsZ *in vivo* (11), we compared FtsZ turnover rates in the wild-type, Δ*minC*, and Δ*clpX* Δ*minC* strains. We performed antibiotic chase experiments and calculated that the half-life of FtsZ in the wild-type strain grown at 30°C is ~140 min (Fig. 5). Unexpectedly, we observed that FtsZ turnover was slower in a Δ*minC* strain than in a wild-type strain; in the 3 h following addition of spectinomycin, only ~20% of the cellular FtsZ was degraded in the Δ*minC* strain, compared with ~60% in the wild-type strain. FtsZ turnover was not significantly slower in the Δ*clpX* Δ*minC*

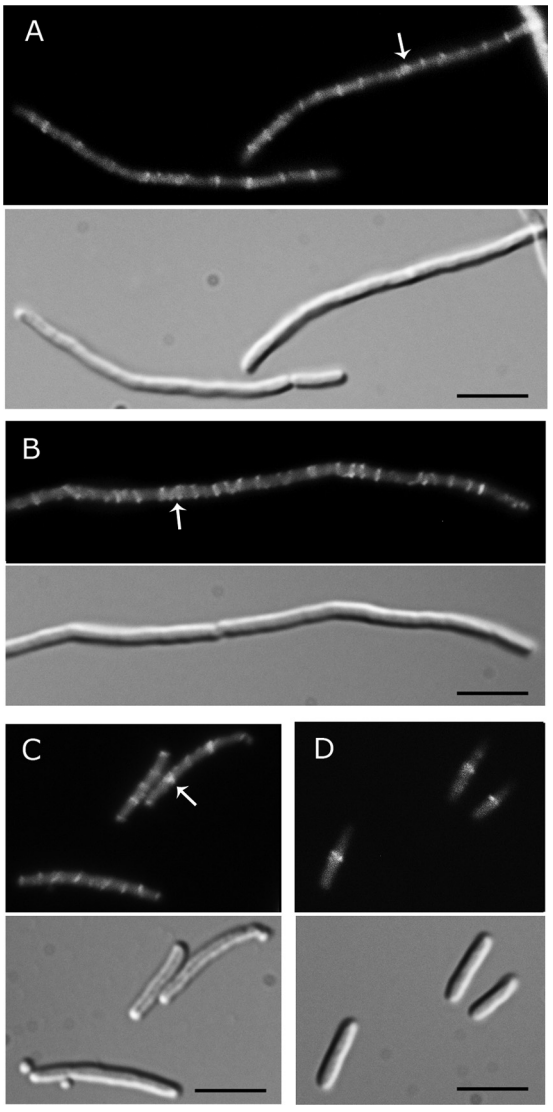

FIG. 4. FtsZ rings are present in long filaments of Δ*clpX* Δ*minC* and Δ*clpP* Δ*minC* cells. Cells expressing plasmid-encoded Gfp-FtsZ were prepared as described in Materials and Methods. FtsZ rings were visible by fluorescence (upper panel) and DIC (lower panel) microscopy in all strains: Δ*clpX* Δ*minC* (A), Δ*clpP* Δ*minC* (B), Δ*minC* (C), and wild-type MG1655 (D). Arrows indicate positions of thick FtsZ bands or adjacent rings. Bars, 5 μm.

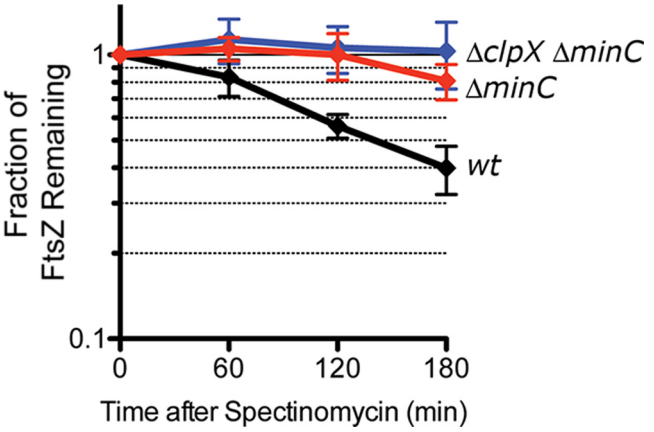

FIG. 5. Deletion of *minC* reduces the rate of FtsZ degradation by ClpXP. FtsZ turnover was calculated by comparing relative FtsZ levels in each strain after addition of spectinomycin and immunoblotting as described in Materials and Methods. Strains tested include wild-type (wt) MG1655, Δ*minC*, and Δ*clpX* Δ*minC*.

strain than in the Δ*minC* strain (Fig. 5). These results suggest that MinC promotes degradation of FtsZ by ClpXP either directly or indirectly.

We compared global levels of FtsZ from cultures in log phase without halting protein synthesis and found no significant differences in the levels of FtsZ in any of the strains tested (see Fig. S6 in the supplemental material). This result is in agreement with previously published work indicating that FtsZ levels do not change significantly in *min* mutants (39).

Since there is slower turnover of FtsZ in Δ*minC* and Δ*minC* Δ*clpX* strains than in a wild-type strain, one possible explanation for synthetic filamentation in the *clp min* double mutant is the persistence of a cell division inhibitor, which is a substrate for ClpXP. Failure to degrade an inhibitor due to deletion of *clpX* or *clpP* could lead to division delay, which may be more pronounced in a *minC* deletion strain, where FtsZ is diluted among multiple ring structures. A second possibility to explain these results is that ClpXP may degrade a subpopulation of FtsZ that is dependent on MinC for localization.

Next, we tested whether increasing the intracellular concentration of FtsZ by expressing FtsZ from a plasmid could suppress the formation of long filaments in Δ*clpX* Δ*minC* and Δ*clpP* Δ*minC* cultures. We observed that overexpression of FtsZ alone, or overexpression of FtsZ, FtsA, and FtsQ from the pZAQ plasmid (data not shown), reduced overall cell length and suppressed the long filament phenotype of Δ*clpX* Δ*minC* and Δ*clpP* Δ*minC* strains (see Fig. S7 in the supplemental material). This result is consistent with the above suggestion that the availability of functional FtsZ is limited in the Δ*clpX* Δ*minC* and Δ*clpP* Δ*minC* strains. However, since multiple cell division abnormalities can be suppressed by overexpression of FtsZ, including those that are synthetic with a *min* deletion, such as *envC* and *slmA*, as well as several cell shape mutants (6–8), the explanation may be more complex.

Model for ClpXP function during cell division. We have shown that prevention of degradation by ClpXP partially suppresses temperature-sensitive filamentation of *ftsZ84* cells and prevents FtsZ84 turnover, suggesting that ClpXP may modulate cell division through FtsZ degradation. We have also shown that deletion of *clpX* or *clpP* in combination with deletion of *minC* causes cell division defects. However, FtsZ degradation is reduced in the Δ*minC* strain compared to the wild-type strain and is not significantly more reduced in the Δ*clpX* Δ*minC* mutant, suggesting that ClpXP may act in cell division by degrading a cell division component other than FtsZ. Together, our results suggest that ClpXP may degrade multiple cell division proteins.

Any model to explain the observations must include a role for ClpX that incorporates ATP-dependent protein unfolding activity and a role for ClpP. Thus, the mechanism of action of ClpX in *B. subtilis* cell division, which involves ATP-independent and ClpP-independent inhibition of FtsZ polymerization (22, 38), is not easily applicable to *E. coli*. However, under

certain conditions for *E. coli* where ClpX is greatly overexpressed independent of ClpP, cell division is perturbed (34), and the mechanism is likely through direct binding of ClpX to FtsZ and prevention of FtsZ polymerization.

One model to explain how ClpXP might modulate cell division, consistent with ClpXP acting directly on FtsZ (11) and FtsZ84 (Fig. 1), is that ClpXP degrades FtsZ, thereby destabilizing the FtsZ ring and allowing FtsZ polymers to undergo necessary remodeling and conformational changes associated with ring constriction and septation. This might occur as the result of FtsZ polymer severing directly through extraction and degradation of FtsZ protomers from the fibers followed by remodeling of the shorter fibers. ClpXP may also degrade free FtsZ protomers, thereby driving the FtsZ monomer-polymer equilibrium in the direction of polymer disassembly. Similar mechanisms of action have been proposed for other Clp and Clp-like proteins, such as disassembly of amyloid fibers by Hsp104 (33) and severing of microtubules by spastin (31). A notable aspect of this model is that very few cycles of FtsZ protomer degradation are required to promote polymer fragmentation, which is consistent with the relatively small amount (10 to 15% per generation) of FtsZ degradation seen *in vivo* (11).

Our data with *minC* double mutants with *clpX* and *clpP* are consistent with a model in which ClpXP promotes degradation of another cell division protein that functions downstream of FtsZ ring assembly, possibly participating in FtsZ ring remodeling, the timing of constriction or the insertion of cell wall components. For example, this unidentified cell division protein could be a division inhibitor that, in the absence of ClpXP, causes a cell division delay, which is more pronounced in a *minC* deletion strain. Alternatively, this unidentified protein might be a cell division component that becomes out of balance with the other components when ClpXP is not present. For example, the levels of FtsZ and FtsA are in balance; increasing FtsA causes cell division inhibition, and the inhibition is relieved by excess FtsZ (14). If FtsA turnover were controlled in a ClpXP-dependent manner, as suggested by a proteomic study (30), then deletion of *clpX* or *clpP* would cause excess FtsA, leading to division inhibition. More complicated models that involve degradation of a subpopulation of FtsZ cannot be ruled out at this time.

Perhaps it is more likely that ClpXP influences cell division by degrading multiple components, thereby modulating the finely balanced interplay of the many factors required for cell division. In *E. coli* there are several cell division components and regulators among the large and diverse set of proteins that have been implicated as potential ClpXP substrates, including MinD and penicillin binding proteins 5 and 6, in addition to FtsZ and FtsA (19, 30).

ACKNOWLEDGMENTS

We thank Susan Gottesman, Kumaran Ramamurthi, and Maria Sandkvist for helpful discussions, Nadim Majdalani for technical assistance, Joe Lutkenhaus for the pZAQ expression plasmid, and Matt Chenoweth for construction of pFtsZ. We are grateful to the reviewers for their insightful comments. We also thank Shannon Doyle, Danielle Johnston, Marie-Caroline Miot, and Olivier Genest for critical reading of the manuscript and helpful discussions.

This research was supported by the Intramural Research Program of the NIH, National Cancer Institute Center for Cancer Research.

REFERENCES

1. **Adams, D. W., and J. Errington.** 2009. Bacterial cell division: assembly, maintenance and disassembly of the Z ring. Nat. Rev. Microbiol. **7:**642–653.
2. **Akerlund, T., R. Bernander, and K. Nordstrom.** 1992. Cell division in *Escherichia coli minB* mutants. Mol. Microbiol. **6:**2073–2083.
3. **Akerlund, T., K. Nordstrom, and R. Bernander.** 1993. Branched *Escherichia coli* cells. Mol. Microbiol. **10:**849–858.
4. **Anderson, D. E., F. J. Gueiros-Filho, and H. P. Erickson.** 2004. Assembly dynamics of FtsZ rings in *Bacillus subtilis* and *Escherichia coli* and effects of FtsZ-regulating proteins. J. Bacteriol. **186:**5775–5781.
5. **Baba, T., et al.** 2006. Construction of *Escherichia coli* K-12 in-frame, single-gene knockout mutants: the Keio collection. Mol. Syst. Biol. **2:**2006.0008.
6. **Bendezu, F. O., and P. A. de Boer.** 2008. Conditional lethality, division defects, membrane involution, and endocytosis in *mre* and *mrd* shape mutants of *Escherichia coli*. J. Bacteriol. **190:**1792–1811.
7. **Bernhardt, T. G., and P. A. de Boer.** 2004. Screening for synthetic lethal mutants in *Escherichia coli* and identification of EnvC (YibP) as a periplasmic septal ring factor with murein hydrolase activity. Mol. Microbiol. **52:** 1255–1269.
8. **Bernhardt, T. G., and P. A. de Boer.** 2005. SlmA, a nucleoid-associated, FtsZ binding protein required for blocking septal ring assembly over chromosomes in *E. coli*. Mol. Cell **18:**555–564.
9. **Bi, E., and J. Lutkenhaus.** 1990. Analysis of *ftsZ* mutations that confer resistance to the cell division inhibitor SulA (SfiA). J. Bacteriol. **172:**5602–5609.
10. **Blattner, F. R., et al.** 1997. The complete genome sequence of *Escherichia coli* K-12. Science **277:**1453–1462.
11. **Camberg, J. L., J. R. Hoskins, and S. Wickner.** 2009. ClpXP protease degrades the cytoskeletal protein, FtsZ, and modulates FtsZ polymer dynamics. Proc. Natl. Acad. Sci. U. S. A. **106:**10614–10619.
12. **Chen, Y., and H. P. Erickson.** 2005. Rapid in vitro assembly dynamics and subunit turnover of FtsZ demonstrated by fluorescence resonance energy transfer. J. Biol. Chem. **280:**22549–22554.
13. **Cherepanov, P. P., and W. Wackernagel.** 1995. Gene disruption in *Escherichia coli*: TcR and KmR cassettes with the option of Flp-catalyzed excision of the antibiotic-resistance determinant. Gene **158:**9–14.
14. **Dai, K., and J. Lutkenhaus.** 1992. The proper ratio of FtsZ to FtsA is required for cell division to occur in *Escherichia coli*. J. Bacteriol. **174:**6145–6151.
15. **Dai, K., Y. Xu, and J. Lutkenhaus.** 1993. Cloning and characterization of *ftsN*, an essential cell division gene in *Escherichia coli* isolated as a multicopy suppressor of *ftsA12*(Ts). J. Bacteriol. **175:**3790–3797.
16. **Dajkovic, A., G. Lan, S. X. Sun, D. Wirtz, and J. Lutkenhaus.** 2008. MinC spatially controls bacterial cytokinesis by antagonizing the scaffolding function of FtsZ. Curr. Biol. **18:**235–244.
17. **de Boer, P. A., R. E. Crossley, and L. I. Rothfield.** 1989. A division inhibitor and a topological specificity factor coded for by the minicell locus determine proper placement of the division septum in *E. coli*. Cell **56:**641–649.
18. **Dziedzic, R., et al.** 2010. *Mycobacterium tuberculosis* ClpX interacts with FtsZ and interferes with FtsZ assembly. PLoS One **5:**e11058.
19. **Flynn, J. M., S. B. Neher, Y. I. Kim, R. T. Sauer, and T. A. Baker.** 2003. Proteomic discovery of cellular substrates of the ClpXP protease reveals five classes of ClpX-recognition signals. Mol. Cell **11:**671–683.
20. **Gottesman, S., W. P. Clark, V. de Crecy-Lagard, and M. R. Maurizi.** 1993. ClpX, an alternative subunit for the ATP-dependent Clp protease of *Escherichia coli*. Sequence and in vivo activities. J. Biol. Chem. **268:**22618–22626.
21. **Guzman, L. M., D. Belin, M. J. Carson, and J. Beckwith.** 1995. Tight regulation, modulation, and high-level expression by vectors containing the arabinose P_{BAD} promoter. J. Bacteriol. **177:**4121–4130.
22. **Haeusser, D. P., A. H. Lee, R. B. Weart, and P. A. Levin.** 2009. ClpX inhibits FtsZ assembly in a manner that does not require its ATP hydrolysis-dependent chaperone activity. J. Bacteriol. **191:**1986–1991.
23. **Hersch, G. L., R. E. Burton, D. N. Bolon, T. A. Baker, and R. T. Sauer.** 2005. Asymmetric interactions of ATP with the AAA+ ClpX6 unfoldase: allosteric control of a protein machine. Cell **121:**1017–1027.
24. **Hoskins, J. R., S. K. Singh, M. R. Maurizi, and S. Wickner.** 2000. Protein binding and unfolding by the chaperone ClpA and degradation by the protease ClpAP. Proc. Natl. Acad. Sci. U. S. A. **97:**8892–8897.
25. **Hu, Z., and J. Lutkenhaus.** 2001. Topological regulation of cell division in E. coli. Spatiotemporal oscillation of MinD requires stimulation of its ATPase by MinE and phospholipid. Mol. Cell **7:**1337–1343.
26. **Ivanov, V., and K. Mizuuchi.** 2010. Multiple modes of interconverting dynamic pattern formation by bacterial cell division proteins. Proc. Natl. Acad. Sci. U. S. A. **107:**8071–8078.
27. **Li, Z., M. J. Trimble, Y. V. Brun, and G. J. Jensen.** 2007. The structure of FtsZ filaments in vivo suggests a force-generating role in cell division. EMBO J. **26:**4694–4708.
28. **Lutkenhaus, J.** 2007. Assembly dynamics of the bacterial MinCDE system and spatial regulation of the Z ring. Annu. Rev. Biochem. **76:**539–562.
29. **Meinhardt, H., and P. A. de Boer.** 2001. Pattern formation in *Escherichia*

coli: a model for the pole-to-pole oscillations of Min proteins and the localization of the division site. Proc. Natl. Acad. Sci. U. S. A. **98:**14202–14207.
30. **Neher, S. B., et al.** 2006. Proteomic profiling of ClpXP substrates after DNA damage reveals extensive instability within SOS regulon. Mol. Cell **22:**193–204.
31. **Roll-Mecak, A., and R. D. Vale.** 2008. Structural basis of microtubule severing by the hereditary spastic paraplegia protein spastin. Nature **451:**363–367.
32. **Sauer, R. T., et al.** 2004. Sculpting the proteome with AAA(+) proteases and disassembly machines. Cell **119:**9–18.
33. **Shorter, J., and S. Lindquist.** 2004. Hsp104 catalyzes formation and elimination of self-replicating Sup35 prion conformers. Science **304:**1793–1797.
34. **Sugimoto, S., et al.** 2010. AAA+ chaperone ClpX regulates dynamics of prokaryotic cytoskeletal protein FtsZ. J. Biol. Chem. **285:**6648–6657.
35. **Tonthat, N. K., et al.** 2011. Molecular mechanism by which the nucleoid occlusion factor, SlmA, keeps cytokinesis in check. EMBO J. **30:**154–164.
36. **Wang, X. D., P. A. de Boer, and L. I. Rothfield.** 1991. A factor that positively regulates cell division by activating transcription of the major cluster of essential cell division genes of *Escherichia coli*. EMBO J. **10:**3363–3372.
37. **Weart, R. B., and P. A. Levin.** 2003. Growth rate-dependent regulation of medial FtsZ ring formation. J. Bacteriol. **185:**2826–2834.
38. **Weart, R. B., S. Nakano, B. E. Lane, P. Zuber, and P. A. Levin.** 2005. The ClpX chaperone modulates assembly of the tubulin-like protein FtsZ. Mol. Microbiol. **57:**238–249.
39. **Yu, X. C., and W. Margolin.** 2000. Deletion of the *min* operon results in increased thermosensitivity of an *ftsZ84* mutant and abnormal FtsZ ring assembly, placement, and disassembly. J. Bacteriol. **182:**6203–6213.
40. **Yu, X. C., and W. Margolin.** 1999. FtsZ ring clusters in *min* and partition mutants: role of both the Min system and the nucleoid in regulating FtsZ ring localization. Mol. Microbiol. **32:**315–326.